

# **NASA TECHNICAL MEMORANDUM**

NASA TM X-64562

## **ON THE RELATIONSHIP BETWEEN SMALL-SCALE WIND SHEARS AND WIND PROFILE POWER SPECTRA**

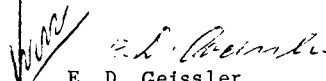
By George H. Fichtl  
Aero-Astroynamics Laboratory

October 27, 1970

# **CASE FILE COPY**

**NASA**

*George C. Marshall Space Flight Center  
Marshall Space Flight Center, Alabama*

1. Report No. NASA TM X-64562		2. Government Accession No.		3. Recipient's Catalog No.	
4. Title and Subtitle ON THE RELATIONSHIP BETWEEN SMALL-SCALE WIND SHEARS AND WIND PROFILE POWER SPECTRA				5. Report Date October 27, 1970	
				6. Performing Organization Code	
7. Author(s) George H. Fichtl				8. Performing Organization Report No.	
9. Performing Organization Name and Address Aerospace Environment Division Aero-Astroynamics Laboratory George C. Marshall Space Flight Center Marshall Space Flight Center, Alabama 35812				10. Work Unit No.	
				11. Contract or Grant No.	
12. Sponsoring Agency Name and Address				13. Type of Report and Period Covered TECHNICAL MEMORANDUM	
				14. Sponsoring Agency Code	
15. Supplementary Notes					
16. Abstract  Rawinsonde wind profile data provide accurate wind shear information for intervals $\Delta z \geq 1$ km. To specify wind shears for $\Delta z < 1$ km for space vehicle design, detailed wind profile information like that provided by the FPS-16 radar/Jimsphere system or an extrapolation procedure is required. This report is concerned with the latter alternative. It is assumed that any realization from an ensemble of wind profiles can be represented in terms of a Fourier integral. This permits the calculation of the ensemble standard deviation and mean of the corresponding shear ensemble for any altitude and shear interval $\Delta z$ in terms of the power spectrum of the ensemble of wind profiles. To calculate how the mean and standard deviations depend on $\Delta z$ , it is assumed that (1) the wind profile power spectrum behaves like $\kappa^{-2.4}$ at sufficiently large values of the vertical wave number $\kappa$ , (2) the vertical variation of the power spectrum can be neglected locally in the calculations of the ensemble mean and standard deviations of the wind shear, and (3) the probability distribution function of the standardized shear variate is invariant with $\Delta z$ . The results of these calculations show that the mean and standard deviations of the shear ensemble, as well as the shear for any percentile, asymptotically behave like $(\Delta z)^{0.7}$ . This result is in excellent agreement with shear data from Cape Kennedy, Florida.					
17. Key Words (Suggested by Author(s))  Wind shear, turbulence, space vehicles structures, aircraft			18. Distribution Statement PUBLIC RELEASE:   E. D. Geissler Director, Aero-Astroynamics Laboratory		
19. Security Classif. (of this report) UNCLASSIFIED		20. Security Classif. (of this page) UNCLASSIFIED		21. No. of Pages 35	
				22. Price*	

#### ACKNOWLEDGEMENTS

The author would like to thank Mr. C. Hill of the Aerospace Environment Division, Aero-Astroynamics Laboratory, Marshall Space Flight Center, for the use of his wind shear data that went into the construction of figures 1-4.

# TABLE OF CONTENTS

	<u>Page</u>
I. INTRODUCTION.....	1
II. ENSEMBLE STANDARD DEVIATION OF WIND SHEAR.....	3
III. ENSEMBLE MEAN WIND SHEAR.....	8
IV. STATISTICALLY HOMOGENEOUS WIND PROFILE ENSEMBLE.....	9
V. NONHOMOGENEOUS WIND PROFILE ENSEMBLE.....	11
VI. EXPERIMENTAL DATA.....	17
VII. CONCLUDING COMMENTS.....	22
APPENDIX A: Proof that the $\phi_r(\kappa, z)$ and $\phi_i(\kappa, z)$ are Even and Odd Functions of $\kappa$ .....	23

# LIST OF SYMBOLS

<u>Symbol</u>	<u>Definition</u>
$B(\kappa)$	Fourier amplitude of the fluctuation portion of a scalar wind profile
$C(\kappa)$	Fourier amplitude of a scalar wind profile at wave number $\kappa$
$F_1$	distribution function of build-up shears
$F_2$	distribution function of back-off shears
$p$	exponent in power law of $\Phi(\kappa)$
$p(x)$	probability density function of $x$
$p_r$	exponent in power law of $\phi_r(\kappa)$
$P$	probability
$q_r$	exponent in power law of $\psi_r(\kappa)$
$s_1$	build-up scalar wind shear fluctuation
$s_2$	back-off scalar wind shear fluctuation
$S_1$	build-up scalar wind shear
$S_2$	back-off scalar wind shear
$v(z)$	scalar wind speed fluctuation relative to the ensemble mean scalar wind profile
$V(z)$	scalar wind speed at height $z$
$V_1$	lower wind speed bound on $V(z_r)$
$V_2$	upper wind speed bound on $V(z_r)$
$x$	standardized shear variate
$z$	altitude
$z_r$	altitude at reference level

# LIST OF SYMBOLS (Cont'd)

<u>Symbol</u>	<u>Definition</u>
$\alpha$	$p_r(z_r)$ or $q_r(z_r)$
$\beta_r$	coefficient of proportionality in power law of $\phi_r$
$\gamma_r$	coefficient of proportionality in power law of $\psi_r$
$\Gamma(\xi)$	gamma function of $\xi$
$\Delta z$	wind shear height interval
$K$	wave number
$\mu_1$	ensemble mean of $S_1$
$\sigma_1$	ensemble standard deviation of $S_1$
$\phi(K, z)$	power spectrum of $v$
$\phi_r(K, z)$	real part of $\phi$
$\phi_i(K, z)$	imaginary part of $\phi$
$\Phi(K)$	homogeneous spectrum of $v$
$\psi(K, z)$	power spectrum of $\langle V \rangle$
$\psi_r(K, z)$	real part of $\psi$
$\psi_i(K, z)$	imaginary part of $\psi$
$\langle ( ) \rangle$	ensemble average of ( )
$( )^*$	complex conjugate of ( )
$( )^+$	quantity associated with a given percentile
$( \vec{\phantom{a}} )$	vector quantity

# ON THE RELATIONSHIP BETWEEN SMALL-SCALE WIND SHEARS AND WIND PROFILE POWER SPECTRA

## SUMMARY

Statistical wind shear information is used in the construction of synthetic wind profiles for the design of space vehicles. In practice, design scalar shears for various wind speed categories at various altitudes at which the shears are to be applied are derived from rawinsonde wind profile data. These data provide wind shear information for intervals equal to and greater than 1 km. To obtain wind shear information for intervals less than 1 km, detailed wind profile information like that obtained from the FPS-16 radar/Jimsphere wind sensing system is required. However, there are space vehicle launch sites which do not have detailed wind profile data in sufficient quantity to calculate statistical design shears. Accordingly, alternative procedures for deriving small-scale wind shears are required. The introduction of suitable hypotheses about the behavior of wind profile spectra at large wave numbers and the invariance of the distribution function of wind shears with regard to varying shear intervals facilitates the derivation of an extrapolation procedure whereby one can extrapolate the rawinsonde shear statistics down into the region of shear intervals which are less than 1 km. To do this, it is assumed that any scalar wind profile from an ensemble of wind profiles can be represented in terms of a Fourier integral. The Fourier integrals permit us to relate the ensemble variance and mean of the wind shears to the power spectrum of the wind profile ensemble. The Fourier representation is general and accounts for the vertical nonhomogeneous statistical properties of the wind profile ensemble. It is hypothesized that (1) the power spectrum of the wind profile behaves like  $\kappa^{-2.4}$  at sufficiently large values of the vertical wave number  $\kappa$ , (2) the vertical variation of the wind profile power spectrum can be neglected locally in the calculation of the ensemble mean and variance of the shear, and (3) the probability distribution function of the standardized shear variate is invariant with shear interval  $\Delta z$ . These hypotheses are used to calculate the asymptotic behavior of wind shear statistics for sufficiently small values of  $\Delta z$ . It is shown that the standard deviation and mean of the shear ensemble, as well as the shear for any percentile level occurrence, behave like  $(\Delta z)^{0.7}$  for sufficiently small values of  $\Delta z$ . This result is in excellent agreement with shear data obtained from FPS-16/Jimsphere wind profiles measured at Cape Kennedy, Florida.

## I. INTRODUCTION

This report is concerned with establishing the relationship between small scale wind shears and detailed wind profile spectra in the first 20 km of the atmosphere. Small scale wind shears are defined here to be vertical differences between the zonal, meridional, or scalar winds over vertical height intervals  $\Delta z < 1$  km. To this list of shears, one could add the vector shear, which is the magnitude of the wind shear vector whose components are the zonal and meridional wind shears. We will confine our discussion in this report to scalar wind shears.

Statistical wind shear information is used in the construction of synthetic wind profiles for the design of space vehicles. A detailed account of how a synthetic wind profile is constructed can be found in reference 1. Within NASA the practice has been to specify design wind shears based on scalar wind shear statistics.\* Moreover, two types of shears are considered: build-up and back-off shears, defined as

$$\text{build-up:} \quad S_1(\Delta z, z) = V(z) - V(z - \Delta z) \quad (1)$$

$$\text{back-off:} \quad S_2(\Delta z, z) = V(z + \Delta z) - V(z), \quad (2)$$

where  $V(z)$  is the scalar wind at height  $z$ . The 99 percentile build-up and back-off shears enveloped over all altitudes are used for the design of space vehicles. To do this, the 99 percentile build-up and back-off shears are calculated from the annual empirical conditional scalar build-up and back-off shear distribution functions

$$\text{build-up:} \quad F_1 = F_1(S_1(\Delta z, z) | V_1 < V(z) < V_2) \quad (3)$$

$$\text{back-off:} \quad F_2 = F_2(S_2(\Delta z, z) | V_1 < V(z) < V_2), \quad (4)$$

where  $V_1$  and  $V_2$  take on assigned values. Usually  $V_2 - V_1 = 10 \text{ m sec}^{-1}$  and  $0 < V_1 < 100 \text{ m sec}^{-1}$ . This corresponds to nine wind speed categories at the reference level  $z$ . The distribution functions  $F_1$  and  $F_2$  are calculated from rawinsonde wind profile data and the smallest value of  $\Delta z = 1$  km. Thus, for example, the design scalar shears for  $\Delta z \geq 1$  km for the Eastern Test Range (ETR) are based on serially complete rawinsonde wind profile data which consist of an eight-year sample of wind profiles spaced 12 hours apart with wind speed and direction specified at 1 km intervals in the vertical up to an altitude of 27 km observed during the period 1956 through 1963. The 99% values of  $S_1(\Delta z, z)$  and

---

\*These shears approximate the vector wind shears for sufficiently large wind speed magnitudes at the reference level  $z$  due to the relatively small directional variation in the wind vector with height at relatively high wind speeds.



$S_2(\Delta z, z)$ ,  $S_1^+(\Delta z, z)$  and  $S_2^+(\Delta z, z)$  say, are calculated at 1 km height intervals between  $z = \Delta z$  and  $z = 20$  km for the build-up shears and at 1 km height intervals between  $z = 0$  and  $z = 20 \text{ km} - \Delta z$  for the back-off shears. The maximum value of  $\Delta z$  is usually 10 km. This, for example, will result in 20 values of  $S_1^+(1 \text{ km}, z)$  for  $\Delta z = 1$  km and 16 values of  $S_2^+(5 \text{ km}, z)$  for  $\Delta z = 5$  km. The design scalar shears are then taken to be the supremum values of  $S_1^+(\Delta z, z)$  and  $S_2^+(\Delta z, z)$ ,  $\sup(S_1^+(\Delta z, z))$  and  $\sup(S_2^+(\Delta z, z))$ , say. These calculations can be performed for various intervals ( $V_1 < V(z) < V_2$ ) of the conditionalizing parameter  $V(z)$ , resulting in two sets of design shear curves. One set will consist of the design build-up scalar shears,  $\sup(S_1^+(\Delta z, z))$ , as functions of  $\Delta z$  for various categories of  $V(z)$ , and the other will consist of the design back-off scalar shears,  $\sup(S_2^+(\Delta z, z))$  also as functions of  $\Delta z$  for various categories of  $V(z)$ .

Because of the response properties of the rawinsonde system and the procedures used to calculate wind speeds from rawinsonde data, the currently available rawinsonde data are not suitable for calculating design wind shear statistics for  $\Delta z < 1$  km. To calculate wind shear statistics for  $\Delta z < 1$  km, one requires detailed wind profile data like that obtained from the Jimsphere/FPS-16 radar wind sensing system. The number of detailed wind profiles from a particular launch site may not be large enough to calculate the required empirical conditional distribution functions, equations (3) and (4). However, it is possible to determine an extrapolation procedure from a smaller sample of detailed wind profiles whereby one can extrapolate the values of  $\sup(S_1^+(\Delta z, z))$  and  $\sup(S_2^+(\Delta z, z))$  calculated with rawinsonde data down into the region  $\Delta z < 1$  km, and thus infer values of design scalar wind shear for vertical scales of distance  $\Delta z < 1$  km.

## II. ENSEMBLE STANDARD DEVIATION OF WIND SHEAR

Let us consider an ensemble of scalar wind speed profiles. Each profile extends over the semi-infinite domain  $0 < z < \infty$ . We select the ensemble of scalar wind profiles  $V(z)$  such that the scalar wind speed at  $z_r$ ,  $V(z_r)$ , in each profile lies in the interval  $V_1 < V(z_r) < V_2$ , where  $V_1$  and  $V_2$  have assigned values. We assume that we can express any wind profile from the ensemble with a Fourier integral

$$V(z) = \int_{-\infty}^{\infty} C(\kappa) e^{-i\kappa z} d\kappa, \quad (5)$$

where the Fourier amplitude  $C(\kappa)$  at wave number  $\kappa$  ( $\text{rad m}^{-1}$ ) is given by

$$C(\kappa) = \frac{1}{2\pi} \int_{-\infty}^{\infty} V(z) e^{i\kappa z} dz. \quad (6)$$

The ensemble average of  $V(z)$  is

$$\langle V(z) \rangle = \int_{-\infty}^{\infty} \langle C(\kappa) \rangle e^{-i\kappa z} d\kappa, \quad (7)$$

where  $\langle \rangle$  denotes the ensemble average operator. Upon subtracting (7) from (5), we obtain the scalar wind fluctuation  $v(z)$  at  $z$  with respect to the ensemble mean scalar wind profile; i.e.,

$$v(z) = \int_{-\infty}^{\infty} [C(\kappa) - \langle C(\kappa) \rangle] e^{-i\kappa z} d\kappa. \quad (8)$$

Thus, any wind profile realization from the ensemble is given by

$$V(z) = \langle V(z) \rangle + v(z). \quad (9)$$

By definition, the build-up and back-off scalar shears associated with the interval  $\Delta z$  are

$$\text{build-up:} \quad S_1(z, \Delta z) = \langle S_1(z, \Delta z) \rangle + s_1(z, \Delta z) \quad (10)$$

$$\text{back-off:} \quad S_2(z, \Delta z) = \langle S_2(z, \Delta z) \rangle + s_2(z, \Delta z), \quad (11)$$

where

$$\left. \begin{aligned} \langle S_1(z, \Delta z) \rangle &= \langle V(z) \rangle - \langle V(z - \Delta z) \rangle \\ \langle S_2(z, \Delta z) \rangle &= \langle V(z + \Delta z) \rangle - \langle V(z) \rangle \\ s_1(z, \Delta z) &= v(z) - v(z - \Delta z) \\ s_2(z, \Delta z) &= v(z + \Delta z) - v(z) \end{aligned} \right\}. \quad (12)$$

In the mathematical treatment that follows we will only consider the buildup scalar wind shears since we can formally obtain the back-off shear from the definition of the buildup shear by replacing  $z$  and  $z - \Delta z$  with  $z + \Delta z$  and  $z$ , respectively. Thus, any result we obtain for the buildup shear can be transformed into a statement about the back-off shear.

We now proceed to calculate the variance of  $s_1(z_r, \Delta z)$ . We can express the fluctuation of the scalar wind shear associated with the reference level  $z_r$  in terms of the Fourier integral

$$s_1(z_r, \Delta z) = \int_{-\infty}^{\infty} B(k'') e^{-ik''z_r} [1 - e^{ik''\Delta z}] dk'', \quad (13)$$

where

$$B(k) = C(k) - \langle C(k) \rangle. \quad (14)$$

We also can express  $s_1$  in terms of the complex conjugate of the Fourier amplitudes  $C^*(k)$ , so that

$$s_1(z_r, \Delta z) = \int_{-\infty}^{\infty} B^*(k) e^{ikz_r} [1 - e^{-ik\Delta z}] dk. \quad (15)$$

By definition  $\langle s_1 \rangle = 0$ , so that the variance of  $s_1$  can be obtained by multiplying (13) and (15) and then performing an ensemble average. This yields

$$\sigma_1^2(z_r, \Delta z) = \int_{-\infty}^{\infty} \int_{-\infty}^{\infty} \langle B^*(k) B(k'') \rangle e^{i(k-k'')z_r} (1 - e^{ik''\Delta z}) (1 - e^{-ik\Delta z}) dk'' dk, \quad (16)$$

where it is understood that  $V_1 < V(z_r) < V_2$ . We can rewrite equation (16) by setting

$$k - k'' = k', \quad (17)$$

so that

$$\sigma_1^2(z_r, \Delta z) = \int_{-\infty}^{\infty} \int_{-\infty}^{\infty} \langle B^*(k) B(k-k') \rangle e^{ik'z_r} (1 - e^{i(k-k')\Delta z}) (1 - e^{-ik\Delta z}) dk' dk. \quad (18)$$

Equation (18) gives the ensemble variance  $\sigma_1^2(z_r, \Delta z)$  of the scalar wind shears as a function of the Fourier amplitudes of the scalar wind field. We will use (18) to obtain an approximate expression for  $\sigma_1(z_r, \Delta z)$  which will enable us to make estimates of the scalar shears for vertical scales  $\Delta z < 1$  km upon specifying the wind shears for  $\Delta z \geq 1$  km for any percentile level of occurrence. This will become clear later.

The power spectrum of  $v(z)$  at altitude  $z$  is

$$\phi(k, z) = \int_{-\infty}^{\infty} \langle B^*(k) B(k-k') \rangle e^{ik'z} dk'. \quad (19)$$

Although the quantity  $\phi(k, z_r)$  is complex, the real and imaginary parts of  $\phi(k, z_r)$ ,  $\phi_r(k, z_r)$ , and  $\phi_i(k, z_r)$  are odd and even functions of  $k$ , respectively (see appendix A). Equation (19) permits us to express (18) in the form

$$\sigma_1^2(z_r, \Delta z) = \int_{-\infty}^{\infty} \phi(k, z) (1 - e^{-ik\Delta z}) dk + \int_{-\infty}^{\infty} \phi(k, z_r - \Delta z) (1 - e^{ik\Delta z}) dk, \quad (20)$$

or in terms of the real and imaginary parts of  $\phi(k, z_r)$  and  $\phi(k, z_r - \Delta z)$ :

$$\begin{aligned} \sigma_1^2(z_r, \Delta z) = & \int_{-\infty}^{\infty} \left\{ [\phi_r(k, z_r) + \phi_r(k, z_r - \Delta z)] [1 - \cos(k\Delta z)] \right. \\ & + [\phi_i(k, z_r - \Delta z) - \phi_i(k, z_r)] \sin(k\Delta z) \left. \right\} dk \\ & + i \int_{-\infty}^{\infty} \left\{ [\phi_i(k, z_r) + \phi_i(k, z_r - \Delta z)] [1 - \cos(k\Delta z)] \right. \\ & + [\phi_r(k, z_r) - \phi_r(k, z_r - \Delta z)] \sin(k\Delta z) \left. \right\} dk. \end{aligned} \quad (21)$$

The imaginary part of this expression vanishes because the integrand of the imaginary part of (21) is an odd function of  $\kappa$  on the interval  $-\infty < \kappa < \infty$ . Thus, the reality of  $\sigma_1^2(z_r, \Delta z)$  is guaranteed and

$$\begin{aligned} \sigma_1^2(z_r, \Delta z) = & \int_{-\infty}^{\infty} \left\{ [\phi_r(\kappa, z_r) + \phi_r(\kappa, z_r - \Delta z)] [1 - \cos(\kappa \Delta z)] \right. \\ & \left. + [\phi_i(\kappa, z_r - \Delta z) - \phi_i(\kappa, z_r)] \sin(\kappa \Delta z) \right\} d\kappa. \end{aligned} \quad (22)$$

If the ensemble of wind profiles has statistically homogeneous properties, then the spectrum of  $v(z)$  is real and independent of position  $z$ . This means that

$$\left. \begin{aligned} \phi(\kappa) &= \phi_r(\kappa, z_r) = \phi_r(\kappa, z_r - \Delta z) \\ \phi_i(\kappa, z_r) &= \phi_i(\kappa, z_r - \Delta z) = 0 \end{aligned} \right\}, \quad (23)$$

so that (22) reduces to

$$\sigma_1^2(\Delta z) = 4 \int_0^{\infty} (1 - \cos(\kappa \Delta z)) \phi(\kappa) d\kappa, \quad (24)$$

where we have used the even properties of  $\phi(\kappa)$  to obtain an integral over the semi-infinite interval  $0 < \kappa < \infty$ . The result given by (24) can also be obtained by noting that  $\phi(\kappa, z)$  can only be independent of  $z$  if

$$\langle B^*(\kappa) B(\kappa - \kappa') \rangle = \phi(\kappa) \delta(\kappa'). \quad (25)$$

Substitution of (25) into (18) yields the result given by (24).

Equation (22) expresses the general relationship between the ensemble variance of the wind shear and the spectrum of  $v(x)$ . Equation (24) is a special case of (22) for the statistical homogeneous case and relates the ensemble variance of the wind shears to the homogeneous power spectrum. We will use these results to infer the dependence of  $\sigma_1(z_r, \Delta z)$  on  $\Delta z$  from the power spectrum of the wind field.

### III. ENSEMBLE MEAN WIND SHEAR

Let us now consider the ensemble mean shear. By definition, the ensemble buildup mean shear associated with the reference height  $z_r$  and the shear interval  $\Delta z$  is

$$\langle S_1(z_r, \Delta z) \rangle = \int_{-\infty}^{\infty} \langle C(k'') \rangle e^{-ik''z_r} (1 - e^{ik''\Delta z}) dk''. \quad (26)$$

Similarly, the ensemble mean shear can be expressed as

$$\langle S_1(z_r, \Delta z) \rangle = \int_{-\infty}^{\infty} \langle C^*(k) \rangle e^{ikz_r} (1 - e^{-ik\Delta z}) dk. \quad (27)$$

Multiplication of (26) and (27) will yield the square of the ensemble mean shear, namely,

$$\begin{aligned} \langle S_1(z_r, \Delta z) \rangle^2 &= \int_{-\infty}^{\infty} \int_{-\infty}^{\infty} \langle C^*(k) \rangle \langle C(k-k') \rangle e^{ik'z_r} (1 - e^{i(k-k')\Delta z}) \\ &\quad \cdot (1 - e^{-ik\Delta z}) dk' dk. \end{aligned} \quad (28)$$

Now the power spectrum of  $\langle V(z) \rangle$  at altitude  $z$  is

$$\psi(k, z) = \int_{-\infty}^{\infty} \langle C^*(k) \rangle \langle C(k-k') \rangle e^{ik'z} dk'. \quad (29)$$

As in the case of the wind shear fluctuations,  $\psi(\kappa, z)$  is complex, and the real and imaginary parts of this function,  $\psi_r(\kappa, z)$  and  $\psi_i(\kappa, z)$ , are even and odd functions of  $\kappa$ , respectively. The proof of this statement is similar to the one in appendix A. Accordingly, the equation for  $\langle S_1(z_r, \Delta z) \rangle^2$  in terms of the real and imaginary parts of  $\psi(\kappa, z)$  can be obtained from (22) by replacing  $\phi_r$ 's and  $\phi_i$ 's in (22) with the corresponding  $\psi_r$ 's and  $\psi_i$ 's, so that

$$\begin{aligned} \langle S_1(z_r, \Delta z) \rangle^2 = \int_{-\infty}^{\infty} \left\{ [\psi_r(\kappa, z_r) + \psi_r(\kappa, z_r - \Delta z)] [1 - \cos(\kappa \Delta z)] \right. \\ \left. + [\psi_i(\kappa, z_r - \Delta z) - \psi_i(\kappa, z_r)] \sin(\kappa \Delta z) \right\} d\kappa. \end{aligned} \quad (30)$$

In the case of statistically homogeneous conditions, the spectrum of  $\langle V(z) \rangle$  is real and independent of  $z$ . Moreover, the spectrum is a delta function, so that

$$\psi_r(\kappa, z_r) = \psi_r(\kappa, z_r - \Delta z) = \langle V \rangle^2 \delta(\kappa) \quad (31)$$

$$\psi_i(\kappa, z_r) = \psi_i(\kappa, z_r) = 0, \quad (32)$$

where  $\langle V \rangle^2$  is the square of the ensemble mean wind profile which is independent of  $z$ . Substitution of (31) and (32) into (30) will show that  $\langle S_1(z_r, \Delta z) \rangle^2$  vanishes for statistically homogeneous conditions.

Equation (30) is the general relationship between the ensemble mean buildup scalar wind shear and the spectrum of the ensemble mean scalar wind profile.

#### IV. STATISTICALLY HOMOGENEOUS WIND PROFILE ENSEMBLE

We have found that, for an ensemble of statistically homogeneous wind profiles, the ensemble mean wind shear vanishes and the variance of the wind shear is given by (24), which we will repeat here for convenience:

$$\sigma_1^2(\Delta z) = 4 \int_0^{\infty} [1 - \cos(\kappa \Delta z)] \Phi(\kappa) d\kappa. \quad (24)$$

It is worthwhile to examine the implication of this formula for spectra that obey power laws. Power spectral calculations with detailed zonal, meridional, and scalar wind profiles observed with the FPS-16/Jimsphere wind-sensing system show that, for sufficiently large wave numbers, the power spectra of individual profiles behave like  $\kappa^{-p}$ , where  $p$  is a positive number with numerical value approximately equal to 2.4 [1,2]. In these calculations the profiles were assumed to be statistically homogeneous. If we invoke the ergodic hypothesis (ensemble averages can be replaced with space averages), then, for sufficiently large wave numbers,

$$\Phi(\kappa) = \beta \kappa^{-p}, \quad (33)$$

where  $\beta$  is a positive quantity that depends on the intensity of the wind fluctuations about the ensemble mean wind profile, which in this case is independent of  $z_r$ .

We wish to calculate the ensemble variance of the shears for small values of  $\Delta z$ ,  $\Delta z < 1$  km, say. Now for sufficiently small values of  $\Delta z$ , the behavior of  $\Phi(\kappa)$  at small wave numbers is relatively unimportant in the evaluation of (24) because the factor  $1 - \cos(\kappa \Delta z)$  in the integrand tends to suppress the contributions to  $\sigma_1^2(\Delta z)$  from  $\Phi(\kappa)$ . Accordingly, we will use (33) to evaluate (24) over the complete interval  $0 < \kappa < \infty$ , so that

$$\sigma_1^2(\Delta z) \approx 4\beta \int_0^{\infty} \kappa^{-p} [1 - \cos(\kappa \Delta z)] d\kappa, \quad (34)$$

or

$$\sigma_1^2(\Delta z) \approx \frac{\beta 2\pi \operatorname{cosec} \left( \frac{1}{2} \pi(p-1) \right)}{(p-1) \Gamma(p-1)} (\Delta z)^{p-1}, \quad (35)$$

provided  $1 < p < 3$ , which corresponds to the situation we are dealing with here. Equation (35) shows that, for statistically homogeneous conditions,



the ensemble standard deviation of the scalar wind shear depends on  $\Delta z$ , asymptotically, like

$$\sigma_1 = \sigma_{1,0} (\Delta z)^{\frac{p-1}{2}}, \quad (36)$$

where

$$\sigma_{1,0} = \left( \frac{2\pi \operatorname{cosec} \left( \frac{1}{2} \pi(p-1) \right)}{(p-1) \Gamma(p-1)} \right)^{1/2} \beta^{1/2}. \quad (37)$$

## V. NONHOMOGENEOUS WIND PROFILE ENSEMBLE

In reality wind profiles are not homogeneous. One example of the nonhomogeneous behavior of wind profiles is the general increase and decrease of the scalar wind speed below and above the core of an atmospheric jet stream. A second example is the change in the eddy structure as height increases through the tropopause; i.e., the wind fluctuations about the running mean of a wind profile realization above the tropopause tend to be larger than the ones below the tropopause, especially when the troposphere is convectively unstable. Gravity wave theory provides a third example. According to Hines [3], the Fourier components

$$\vec{u}(\vec{k}, \vec{x}, t)$$

of the zonal and meridional wind at position  $x$ , and time  $t$  in a gravity wave are given by

$$\vec{u}(\vec{k}, \vec{x}, t) = U(\vec{k}, \omega(\vec{k})) e^{z/2H} e^{i(\vec{k} \cdot \vec{x} - \omega(\vec{k})t)}, \quad (38)$$

where  $\vec{k}$  is a wave number vector,  $H$  is the atmospheric scale height, and  $\omega(\vec{k})$  is the eigen frequency associated with  $\vec{k}$ . The quantity  $Ue^{z/2H}$  is the Fourier amplitude. Hines [3] obtained this solution of the inviscid hydrodynamic equations by perturbing a quiescent isothermal atmosphere with infinitesimal perturbations. The important point here is that Hines' gravity waves constitute one plausible class of motions in the atmosphere which have Fourier amplitudes that increase with altitude like  $e^{z/2H}$ , thus rendering the process nonhomogeneous. There are other types of plausible atmospheric wave motions that have Fourier components that vary with

height in a manner similar to Hines' gravity waves. In view of the obvious nonhomogeneous nature of atmospheric wind profiles, it is reasonable to inquire about how the variance and mean of the scalar wind shear depends on  $\Delta z$ . Unfortunately, the vertical variation of the power spectra of wind profiles is not well known. However, by making assumptions about how  $\phi(\kappa, z)$  and  $\psi(\kappa, z)$  depend on  $\kappa$  and  $z$ , we can make inferences about how  $\sigma_1(z_r, \Delta z)$  and  $\langle S_1(z_r, \Delta z) \rangle$ , which we shall denote with  $\mu_1$ , depend on  $\Delta z$ . Furthermore, the introduction of an assumption concerning the behavior of the probability density function of  $S_1(z, \Delta z)$  as  $\Delta z$  decreases will permit us to predict how  $S_1(z, \Delta z)$  for any percentile depends on  $\Delta z$ . The resulting predictions can be tested with existing experimental data on the distribution function of wind shears from Cape Kennedy, Florida.

The integrands of (22) and (30) are even functions of  $\kappa$ , so that we can replace the integrals over the interval  $-\infty < \kappa < \infty$  with integrals over the interval  $0 < \kappa < \infty$ ; thus,

$$\begin{aligned} \sigma_1^2(z_r, \Delta z) = 2 \int_0^{\infty} \left\{ [\phi_r(\kappa, z_r) + \phi_r(\kappa, z_r - \Delta z)][1 - \cos(\kappa \Delta z)] \right. \\ \left. + [\phi_i(\kappa, z_r - \Delta z) - \phi_i(\kappa, z_r)] \sin(\kappa \Delta z) \right\} d\kappa. \end{aligned} \quad (39)$$

$$\begin{aligned} \mu_1^2(z_r, \Delta z) = 2 \int_0^{\infty} \left\{ [\psi_r(\kappa, z_r) + \psi_r(\kappa, z_r - \Delta z)][1 - \cos(\kappa \Delta z)] \right. \\ \left. + [\psi_i(\kappa, z_r - \Delta z) - \psi_i(\kappa, z_r)] \sin(\kappa \Delta z) \right\} d\kappa. \end{aligned} \quad (40)$$

As stated previously, we do not know how  $\phi(\kappa, z)$  and  $\psi(\kappa, z)$  depend on  $z$ . However, we do know that these quantities are functions of altitude, and this means that there will be different spectra or sorting by wave number for each value of  $z$ . Nevertheless, the process described is a physical one, and we hope that the variation of the spectra from position to position will not be too abrupt, but rather even with smooth variation. With this philosophy in mind, we expand  $\phi_r(\kappa, z_r - \Delta z)$ ,  $\phi_i(\kappa, z_r - \Delta z)$ ,  $\psi_r(\kappa, z_r - \Delta z)$  and  $\psi_i(\kappa, z_r - \Delta z)$  in Taylor's series about the point  $z = z_r$  for small values of  $\Delta z$  so that second- and higher-order terms can be neglected. This permits us to express (39) and (40) as

$$\sigma_1^2(z_r, \Delta z) = 4 \int_0^\infty \phi_r(\kappa, z_r) \left\{ \left[ 1 - \frac{\phi_r'(\kappa, z_r)}{2\phi_r(\kappa, z_r)} \Delta z \right] [1 - \cos(\kappa \Delta z)] - \frac{\phi_i'(\kappa, z_r)}{2\phi_r(\kappa, z_r)} \Delta z \sin(\kappa \Delta z) \right\} d\kappa, \quad (41)$$

$$\mu_1^2(z_r, \Delta z) = 4 \int_0^\infty \psi_r(\kappa, z_r) \left\{ \left[ 1 - \frac{\psi_r'(\kappa, z_r)}{2\psi_r(\kappa, z_r)} \Delta z \right] [1 - \cos(\kappa \Delta z)] - \frac{\psi_i'(\kappa, z_r)}{2\psi_r(\kappa, z_r)} \Delta z \sin(\kappa \Delta z) \right\} d\kappa, \quad (42)$$

where prime denotes differentiation with respect to  $z$ .

If we now assume that

$$\left| \frac{\phi_r'(\kappa, z_r)}{2\phi_r(\kappa, z_r)} \Delta z \right| \ll 1 \quad (43)$$

$$\left| \frac{\phi_i'(\kappa, z_r)}{2\phi_r(\kappa, z_r)} \Delta z \right| \ll 1 \quad (44)$$

$$\left| \frac{\psi_r'(\kappa, z_r)}{2\psi_r(\kappa, z_r)} \Delta z \right| \ll 1 \quad (45)$$

$$\left| \frac{\psi_i'(\kappa, z_r)}{2\psi_r(\kappa, z_r)} \Delta z \right| \ll 1. \quad (46)$$

We can then approximate (41) and (42) as

$$\sigma_1^2(z_r, \Delta z) = 4 \int_0^\infty \phi_r(\kappa, z_r) (1 - \cos(\kappa \Delta z)) d\kappa, \quad (47)$$

$$\mu_1^2(z_r, \Delta z) = 4 \int_0^\infty \psi_r(\kappa, z_r) (1 - \cos(\kappa \Delta z)) d\kappa. \quad (48)$$

The result given by (47) is similar in form to the one for the statistically homogeneous case; however, (47) permits  $\phi_r(\kappa, z_r)$  to vary with  $z_r$ , but the variation must be sufficiently slow such that (43) and (44) are satisfied. Note that, in the nonhomogeneous case,  $\mu_1(z_r, \Delta z)$  is a function of  $z_r$  and  $\Delta z$ , while in the homogeneous case,  $\mu_1$  is equal to zero.

We now assume that, for sufficiently large wave numbers,  $\phi_r(\kappa, z_r)$  and  $\psi_r(\kappa, z_r)$  depend on  $\kappa$  through power laws of the form

$$\phi_r(\kappa, z) = \beta_r(z) \kappa^{-p_r(z)}, \quad (49)$$

$$\psi_r(\kappa, z) = \gamma_r(z) \kappa^{-q_r(z)}, \quad (50)$$

where  $\beta_r$ ,  $\gamma_r$ ,  $p_r$ , and  $q_r$  are positive definite functions of  $z$ . Substitution of (49) and (50) into (47) and (48) yields

$$\sigma_1^2(z_r, \Delta z) = \frac{\beta_r(z_r) 2\pi \operatorname{cosec}(\frac{1}{2} \pi(p_r(z_r)-1))}{(p_r(z_r)-1) \Gamma(p_r(z_r)-1)} (\Delta z)^{p_r(z_r)-1}, \quad (51)$$

$$\mu_1^2(z_r, \Delta z) = \frac{\gamma_r(z_r) 2\pi \operatorname{cosec}(\frac{1}{2} \pi(q_r(z_r)-1))}{(q_r(z_r)-1) \Gamma(q_r(z_r)-1)} (\Delta z)^{q_r(z_r)-1}. \quad (52)$$

These results show that  $\sigma_1 \propto (\Delta z)^{(p_r-1)/2}$  and  $\mu_1 \propto (\Delta z)^{(q_r-1)/2}$  for sufficiently small values of  $\Delta z$ .

Various investigators have experimentally examined the nature of the dependencies of  $\mu_1$  and  $\sigma_1$  on  $\Delta z$ . Adelfang, Ashburn, and Court [4] have shown that the annual climatological mean and standard deviations of the vector shear at Cape Kennedy, Florida, depend on the reference level  $z_r$  and  $\Delta z$ . In particular, they found that both the mean and standard deviations are proportional to  $(\Delta z)^{2/3}$  and the coefficients of proportionality are functions of height. Their analysis was based on 1194 Cape Kennedy Jimsphere profiles. The computations were made at  $z_r = 8, 12$  and  $16$  km for  $\Delta z = 50$  to  $5000$  m. Other authors have deduced power law relationships between  $\Delta z$  and  $\mu_1$  and  $\sigma_1$  (see, for example, references 5 and 6). In view of the results of Adelfang, Ashburn, and Court, we will set

$$p_r(z_r) = q_r(z_r) = \alpha, \quad (53)$$

where  $\alpha$  is a constant. As mentioned previously in Section IV, power spectra of individual scalar wind profiles behave like  $\kappa^{-p}$  at sufficiently large wave numbers, where  $p$  has numerical value approximately equal to 2.4. If we assume that this value of  $p$  obtained from individual profiles can be identified with  $\alpha$ , then  $\alpha - 1 = 1.4$ . Thus, we hypothesize that

$$\begin{aligned} \mu_1(z_r, \Delta z) &\propto (\Delta z)^{0.7} \\ \sigma_1(z_r, \Delta z) &\propto (\Delta z)^{0.7}, \end{aligned} \quad (54)$$

where the coefficients of proportionality are functions of  $z_r$ .

Let us now assume that the conditional probability density function of  $S_1$  can be transformed into the conditional probability density function:

$$p = p(x \mid V_1 < V(z_r) < V_2), \quad (55)$$

where  $x$  is the nondimensional variable:

$$x = \frac{S_1(z_r, \Delta z) - \mu_1(z_r, \Delta z)}{\sigma_1(z_r, \Delta z)}. \quad (56)$$

Integration of (56) over the interval  $-\infty < x < x^+$  will yield probability  $P$  that  $x \leq x^+$ , given that  $V_1 < V(z_r) \leq V_2$ ; i.e.,

$$P(x \leq x^+ | V_1 < V(z_r) \leq V_2) = \int_{-\infty}^{x^+} p(x | V_1 < V(z_r) \leq V_2) dx. \quad (57)$$

Now

$$P(x \leq x^+ | V_1 < V(z_r) \leq V_2) = P(S_1 \leq S_1^+ | V_1 < V(z_r) \leq V_2), \quad (58)$$

where  $S_1^+$  is the value of  $S_1$  associated with  $x^+$ , so that the value of  $S_1^+$  for an assigned value of  $P$  can be obtained by solving (56) for  $S_1^+$  with  $x = x^+$ ; i.e.,

$$S_1^+(z_r, \Delta z) = \mu_1(z_r, \Delta z) + x^+ \sigma_1(z_r, \Delta z). \quad (59)$$

If we now assume that the distribution function of  $x$  is invariant with  $\Delta z$  for a fixed value of  $z_r$ , then it follows that  $x^+$  is only a function of  $P$ , and we conclude from (54) and (59) that

$$S_1^+(z_r, \Delta z) = G(z_r, P(x \leq x^+ | V_1 < V(z_r) \leq V_2)) (\Delta z)^{0.7}, \quad (60)$$

where  $G$  is a function of  $z_r$  and  $P$ . To obtain the design buildup wind shear, we select the supremum value of  $S_1^+(z_r, \Delta z)$  for  $P = 0.99$  from the set of 99 percentile buildup shears that is obtained by letting  $z_r$  take on all permissible values. In view of the hypothesis that  $G$  is independent of  $\Delta z$ , it follows that  $\sup(S_1^+(z_r, \Delta z))$  is proportional to  $(\Delta z)^{0.7}$ . The results given by (51), (52), and (60) also hold for the back-off shears.

## VI. EXPERIMENTAL DATA

To verify the theoretical speculations and hypotheses presented in the previous sections, Mr. C. Hill of the Aerospace Environment Division has made available his calculations of the distribution functions of scalar wind buildup and back-off shears for Cape Kennedy, Florida. Hill performed his calculations with a sample of approximately 256 FPS-16 radar/Jimsphere profiles observed during the period January 3, 1967 to June 30, 1967. The reference levels for his calculations were  $z_r = 1, 2, \dots, 15$  km. At each of these reference levels, he stratified the profiles into  $10 \text{ m sec}^{-1}$  wind speed categories such that  $V_2 - V_1 = 10 \text{ m sec}^{-1}$  and  $V_2 = 10, 20, 30, \dots$ . He then calculated the buildup and back-off shears for each wind speed category for each value of  $z_r = 1, 2, \dots, 15$  km.

Generally, his results show that the buildup and back-off shears for any particular percentile are functions of altitude, and increase like  $(\Delta z)^{0.7}$  for sufficiently small values of  $\Delta z$ ; i.e.,  $\Delta z < 1 - 2$  km. The results for  $z_r = 10$  km for  $10 < V(z_r) \leq 20 \text{ m sec}^{-1}$  and  $30 < V(z_r) \leq 40 \text{ m sec}^{-1}$  were selected for presentation here, and they are typical examples. Figures 1 and 2 contain the buildup shears, and figures 3 and 4 contain the corresponding back-off shears. The figures show that the shear for a given percentile varies like  $(\Delta z)^{0.7}$  for  $\Delta z \leq 1$  km. These results seem to verify the speculations and hypotheses presented in the previous sections: (1) The ensemble fluctuation spectrum and the spectrum of the ensemble mean wind profile are sufficiently slowly varying functions, such that  $\phi_r(k, z_r - \Delta z) \approx \phi_r(k, z_r)$ , etc. for sufficiently small values of  $\Delta z$ , (2) the real parts of the power spectra depend on wave number like  $k^{-2.4}$ , and (3) the distribution function of the standardized shears  $(S_1 - \mu_1)/\sigma_1$  and  $(S_2 - \mu_2)/\sigma_2$  are invariant with  $\Delta z$ .

The fact that  $S_1^+$  and  $S_2^+$  behave like  $(\Delta z)^{0.7}$  for sufficiently small values of  $\Delta z$  permits the estimation of small scale wind shear for  $\Delta z < 1$  km with rawinsonde wind shear data at  $\Delta z = 1$  km. The procedure consists of specifying  $\Delta z$  and calculating the associated shear with the formula

$$S_{1,2}^+(z_r, \Delta z) = S_{1,2}^+(z_r, 1 \text{ km}) (\Delta z)^{0.7}, \quad (61)$$

where  $\Delta z$  is in units of kilometers.

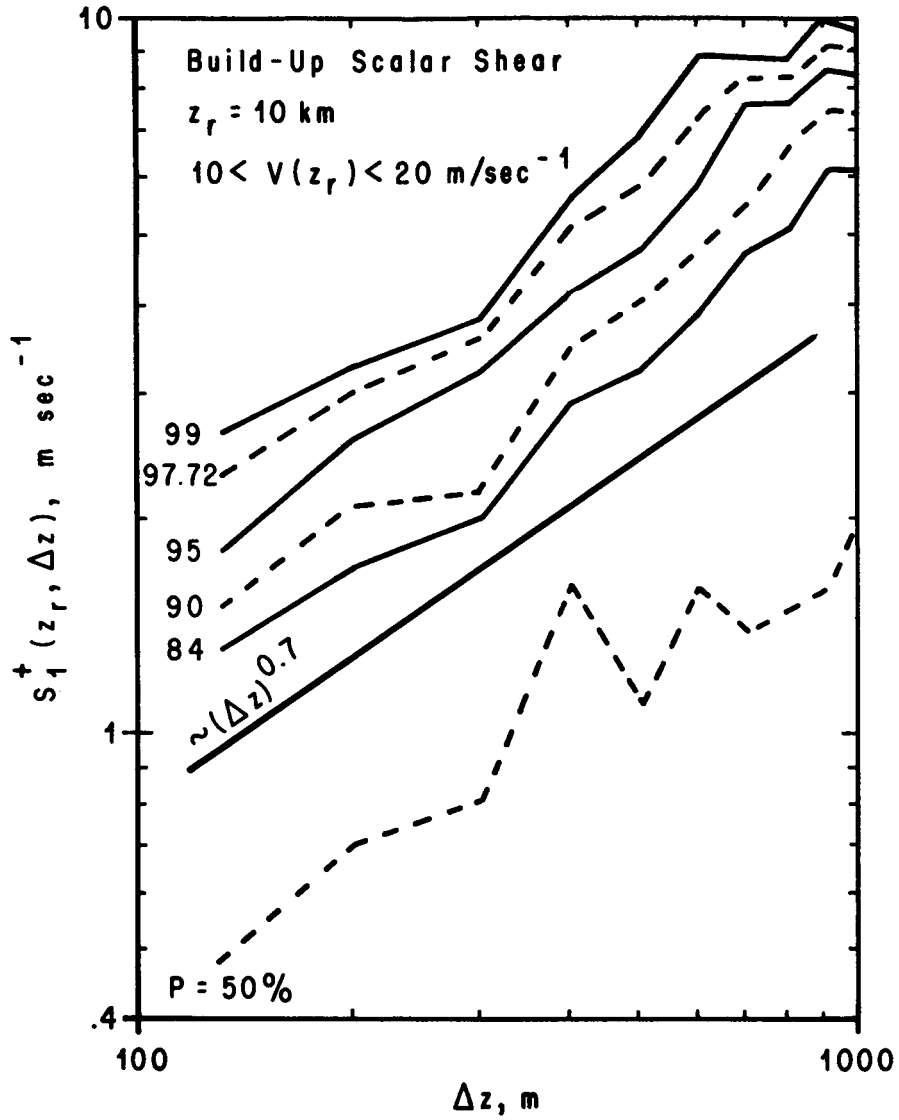


Figure 1. Cape Kennedy, Florida buildup scalar shears  $S_1^+(z_r, \Delta z)$  as functions of  $\Delta z$  for  $z_r = 10 \text{ km}$  and  $10 < V(z_r) \leq 20 \text{ m sec}^{-1}$  for various percentiles.



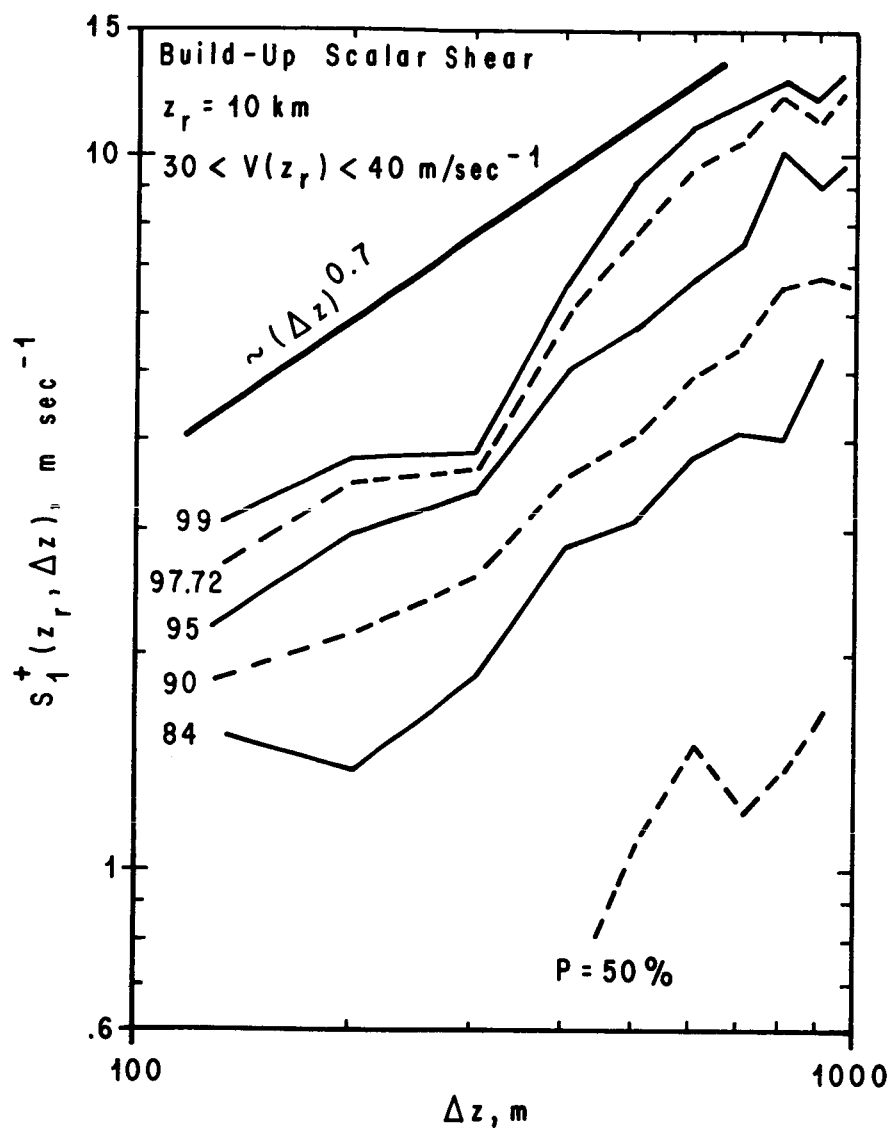


Figure 2. Cape Kennedy, Florida buildup scalar shear  $S_1^+(z_r, \Delta z)$  as functions of  $\Delta z$  for  $z_r = 10 \text{ km}$  and  $30 < V(z_r) \leq 40 \text{ m sec}^{-1}$  for various percentiles.

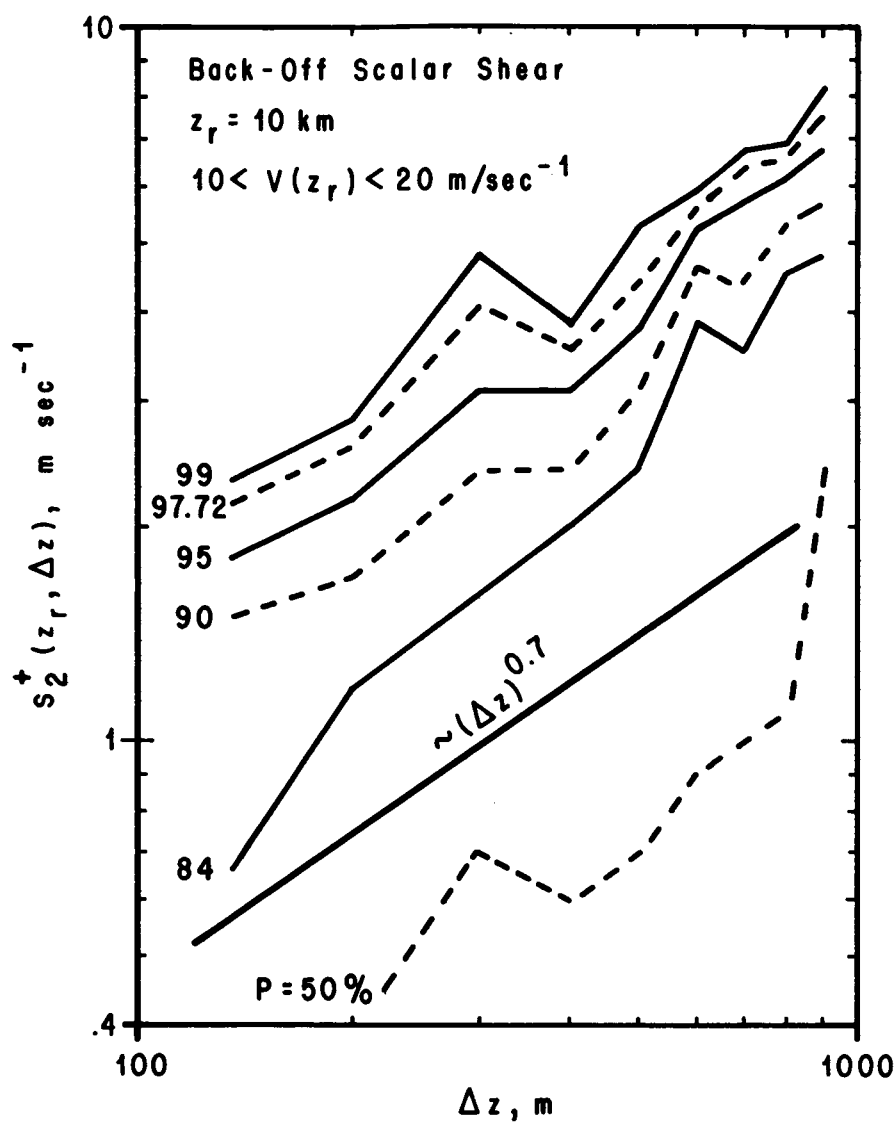


Figure 3. Cape Kennedy, Florida back-off scalar shears  $S_2^+(z_r, \Delta z)$  as functions of  $\Delta z$  for  $z_r = 10 \text{ km}$  and  $10 < V(z_r) \leq 20 \text{ m sec}^{-1}$  for various percentiles.

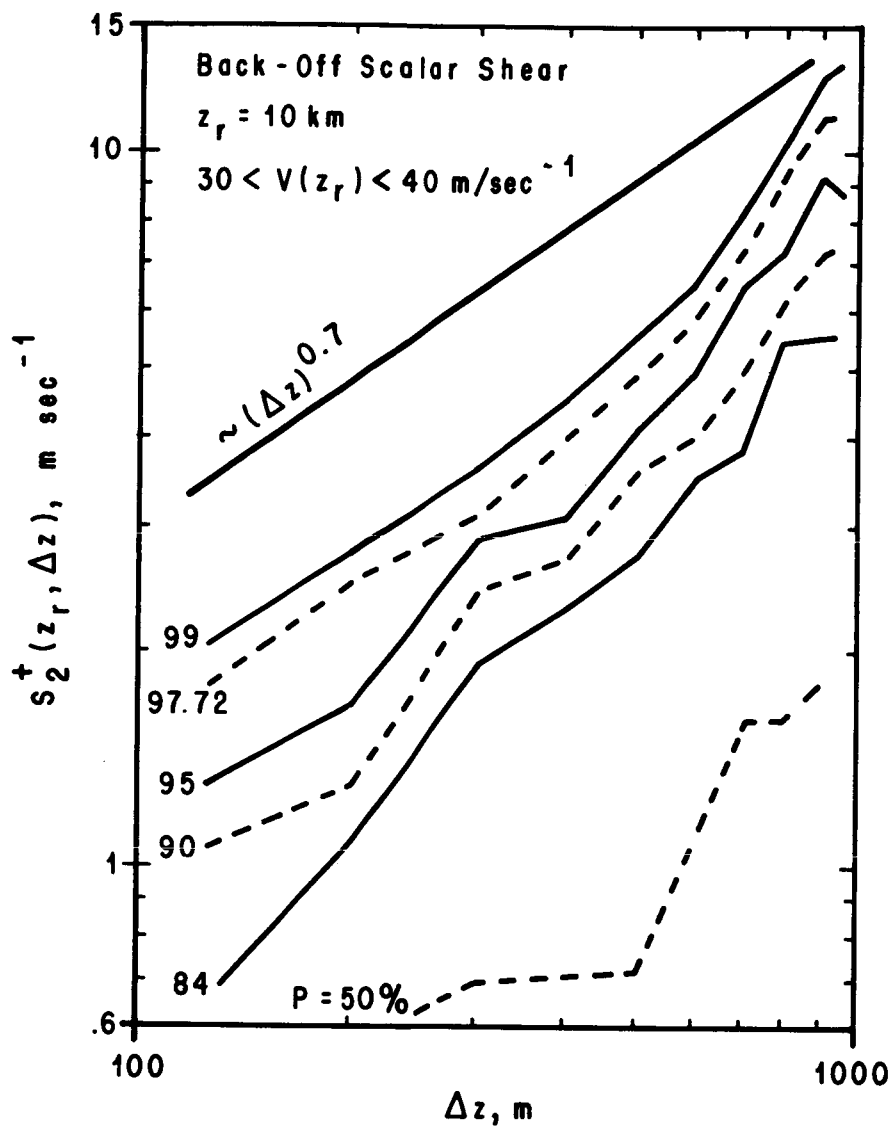


Figure 4. Cape Kennedy, Florida backoff scalar shears  $S_2^+(z_r, \Delta z)$  as functions of  $\Delta z$  for  $z_r = 10 \text{ km}$  and  $30 < V(z_r) \leq 40 \text{ m sec}^{-1}$  for various percentiles.

## VII. CONCLUDING COMMENTS

The purpose of this report has been to determine the relationship between scalar wind shears and power spectra of atmospheric flows. We have seen that there is an intimate relationship between the ensemble mean shear and the spectrum of the ensemble mean wind profile and similarly between the ensemble standard deviation of wind shear and the spectrum of the wind fluctuations relative to the ensemble mean wind profile. The analysis accounted for the nonhomogeneous aspects of wind shear statistics, and in this respect the analysis is general. The hypotheses listed in Section VI enabled us to make relatively accurate predictions about how the buildup and back-off shears vary with  $\Delta z$  for a given percentile level of occurrence. In particular, we found that the scalar wind shears depend on  $\Delta z$  like  $(\Delta z)^{0.7}$  for sufficiently small values of  $\Delta z$ . The analysis in this report can be applied to zonal and meridional wind shears by making slight changes in notation.

## APPENDIX A

Proof that the  $\phi_r(\kappa, z)$  and  $\phi_i(\kappa, z)$  are Even and Odd Functions of  $\kappa$

We assume that  $v(z)$  can be expressed as

$$v(z) = \int_{-\infty}^{\infty} B(\kappa_2) e^{-i\kappa_2 z} dz, \quad (A-1)$$

where

$$B(\kappa_2) = \frac{1}{2\pi} \int_{-\infty}^{\infty} v(z) e^{i\kappa_2 z} dz \quad (A-2)$$

and  $\kappa_2$  is a wave number. The complex conjugate of  $B(\kappa)$  evaluated at wave number  $\kappa_1$  is

$$B^*(\kappa_1) = \frac{1}{2\pi} \int_{-\infty}^{\infty} v(\xi) e^{-i\kappa_1 \xi} d\xi. \quad (A-3)$$

Multiplication of (A-2) and (A-3) and ensemble averaging the resulting relationship yields

$$\langle B^*(\kappa_1) B(\kappa_2) \rangle = \frac{1}{(2\pi)^2} \int_{-\infty}^{\infty} \int_{-\infty}^{\infty} \langle v(z) v(\xi) \rangle e^{i(\kappa_2 z - \kappa_1 \xi)} dz d\xi. \quad (A-4)$$

Complex conjugation of (A-4) yields

$$\langle B^*(\kappa_1) B(\kappa_2) \rangle^* = \frac{1}{(2\pi)^2} \int_{-\infty}^{\infty} \int_{-\infty}^{\infty} \langle v(z) v(\xi) \rangle e^{-i(\kappa_2 z - \kappa_1 \xi)}. \quad (A-5)$$

The right side of (A-5) is  $\langle B^*(-\kappa_1)B(-\kappa_2) \rangle$ . Therefore, we have

$$\langle B^*(\kappa_1)B(\kappa_2) \rangle^* = \langle B^*(-\kappa_1)B(-\kappa_2) \rangle. \quad (\text{A-6})$$

Complex conjugation of (A-6) yields

$$\langle B^*(\kappa_1)B(\kappa_2) \rangle = \langle B^*(-\kappa_1)B(\kappa_2) \rangle^*. \quad (\text{A-7})$$

Now the power spectrum of  $v(z)$  at wave number  $\kappa$  and altitude  $z$  is

$$\phi(\kappa, z) = \int_{-\infty}^{\infty} \langle B^*(\kappa)B(\kappa - \kappa') \rangle e^{i\kappa'z} d\kappa'. \quad (\text{A-8})$$

The corresponding spectrum at wave number  $-\kappa$  is

$$\phi(-\kappa, z) = \int_{-\infty}^{\infty} \langle B^*(-\kappa)B(-\kappa - \kappa') \rangle e^{i\kappa'z} d\kappa'. \quad (\text{A-9})$$

Complex conjugation of (A-9) and utilization of (A-7) yields

$$\phi^*(-\kappa, z) = \int_{-\infty}^{\infty} \langle B^*(\kappa)B(\kappa + \kappa') \rangle e^{-i\kappa'z} d\kappa'. \quad (\text{A-10})$$

Let

$$\kappa' = -\kappa''. \quad (\text{A-11})$$

Thus, (A-10) can be written as

$$\phi^*(-\kappa, z) = \int_{-\infty}^{\infty} \langle B^*(\kappa) B(\kappa - \kappa'') \rangle e^{i\kappa'' z} d\kappa''. \quad (\text{A-12})$$

However,  $\kappa''$  is a dummy variable of integration which we can replace with  $\kappa'$  in (A-12), so that

$$\phi^*(-\kappa, z) = \int_{-\infty}^{\infty} \langle B^*(\kappa) B(\kappa - \kappa') \rangle e^{i\kappa' z} d\kappa'. \quad (\text{A-13})$$

The right-hand sides of equations (A-8) and (A-13) are equal. This means that

$$\phi(\kappa, z) = \phi^*(-\kappa, z), \quad (\text{A-14})$$

from which we conclude

$$\phi_r(\kappa, z) = \phi_r(-\kappa, z) \quad (\text{A-15})$$

$$\phi_i(\kappa, z) = -\phi_i(-\kappa, z). \quad (\text{A-16})$$

Equations (A-15) and (A-16) state that the real and imaginary parts of  $\phi$ ,  $\phi_r$ , and  $\phi_i$  are even and odd functions of  $\kappa$ , respectively.

## REFERENCES

1. Daniels, G. E., "Terrestrial Environment (Climatic) Criteria Guidelines for Use in Space Vehicle Development, 1969 Revision," NASA TM X-53872, NASA-Marshall Space Flight Center, Alabama, May 12, 1969.
2. Fichtl, G. H., D. Camp, and W. W. Vaughan, "Detailed Wind and Temperature Profiles in Clear Air Turbulence and Detection," edited by Hih-Ho Pao and A. Goldberg, Plenum Press, New York, 308, 1969.
3. Hines, C. O., "Internal Atmospheric Gravity Waves at Ionospheric Heights," Can. J. Phys., 38, 1441, 1960.
4. Adelfang, S. I., E. V. Ashburn, and A. Court, "A Study of Jimsphere Wind Profiles as Related to Space Vehicle Design and Operations," Lockheed-California, Burbank, California, NASA CR-1204, Marshall Space Flight Center, Alabama, November 1968.
5. Essenwanger, O., "On the Derivation of Frequency Distributions of Vector Wind Shear for Small Shear Intervals," Geofis. Pura. Appl., 56, 216, 1963.
6. Armendariz, M. and L. J. Rider, "Wind Shear for Small Thickness Layers," J. Appl. Meteor., 5, 810, 1966.



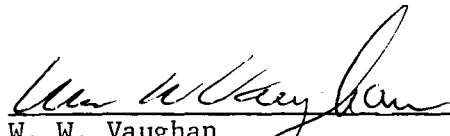
APPROVAL

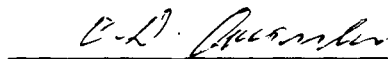
ON THE RELATIONSHIP BETWEEN SMALL-SCALE WIND SHEARS  
AND WIND PROFILE POWER SPECTRA

by George H. Fichtl

The information in this report has been reviewed for security classification. Review of any information concerning Department of Defense or Atomic Energy Commission programs has been made by the MSFC Security Classification Officer. This report, in its entirety, has been determined to be unclassified.

This document has also been reviewed and approved for technical accuracy.

  
\_\_\_\_\_  
W. W. Vaughan  
Chief, Aerospace Environment Division

  
\_\_\_\_\_  
E. D. Geissler  
Director, Aero-Astroynamics Laboratory

## DISTRIBUTION

DIR  
DEP-T  
A&TS-PAT  
PM-PR-M, Mr. Goldston  
A&TS-MS-H  
A&TS-MS-IP  
A&TS-MS-IL (8)  
A&TS-TU, Mr. Wiggins (6)

PM-MO-MGR  
Dr. Speer

S&E-R  
Dr. Johnson

AD-S  
Dr. Stuhlinger

S&E-ASTN  
Mr. Heimbarg  
Mr. Kroll  
Mr. Hunt  
Mr. Showers  
Mr. Moore  
Mr. Stevens

S&E-COMP  
Dr. Hoelzer  
Mrs. McAllister  
Mr. C. Houston

PD-DIR  
Dr. Lucas  
Mr. E. Goerner

S&E-ASTR  
Mr. Mink  
Mr. Hosenthien  
Mr. B. Moore

S&E-CSE  
Dr. Haeussermann  
Mr. Blackstone

S&E-AERO  
Dr. Geissler  
Mr. Horn  
Mr. Dahm  
Mr. Holderer  
Mr. Reed  
Mr. Craighead  
Mr. Rheinfurth  
Mr. Ryan (2)  
Mr. T. Deaton  
Mr. Lindberg  
Mr. Stone  
Mr. Baker  
Mr. Blair  
Mr. Redus  
Mr. Sims  
Dr. Lovingood  
Mr. Cremin  
Mr. Murphree  
Mr. C. Brown  
Mr. Daniels  
Mr. Kaufman (2)  
Mr. Fichtl (25)  
Mr. O. Smith  
Mr. R. Smith  
Mr. W. Vaughan (3)  
Mr. Turner  
Mr. Camp  
Mr. Susko  
Mr. Hill (3)  
Mrs. Alexander  
Mr. MacKiernan  
Mr. Nelson  
Mr. Huffaker  
Mrs. Hightower  
Mr. E. Weaver

NASA-Kennedy Space Center  
Kennedy Space Center, FL 32931  
Attn: Dr. Bruns  
Mr. M. Preston  
Mr. R. Clark  
Library (2)

Sci. & Tech. Info. Facility (25)  
P. O. Box 33  
College Park, Md. 20740  
Attn: NASA Rep. (S-AK/RKT)

NASA-Langley Research Center  
Langley Field, Va.  
Attn: Mr. W. Reed, III  
Mr. R. Steiner  
Mr. H. Runyun  
Mr. H. Tolefson  
Mr. V. Alley  
Library (2)

NASA-Lewis Research Center  
21000 Brookpark Rd.  
Cleveland, Ohio 44135  
Attn: Mr. J. C. Estes  
Library (2)

NASA-Manned Spacecraft Center  
Houston, Texas 77001  
Attn: Mr. D. Wade  
Mr. A. Mackey  
Library (2)

NASA-Headquarters  
Ofc. of Adv. Res. & Tech.  
Washington, D. C. 20546  
Attn: Mr. M. Ames  
Mr. D. Michael  
Mr. W. McGowin  
Mr. M. Charak  
Mr. Tischler

NASA-Flight Research Center  
Box 273  
Edwards AFB, Calif. 93523  
Attn: Director  
Mr. L. J. Ehernberger  
Library (2)

NASA Hdqs.  
Dir. Ofc. of Space Sci. & Appl.  
Washington, D. C. 20546  
Attn: Dr. Morris Tepper

NASA-Goddard Space Flight Center  
Greenbelt, Md. 20771  
Attn: Library (2)

NASA-Ames Res. Center  
Moffett Field, Calif. 94035  
Attn: Library (2)

NASA-Wallops Sta.  
Wallops Island, Va.  
Attn: Library (2)

NASA-Hdqs.  
Ofc. of Manned Space Flight  
Washington, D. C. 20546  
Attn: Mr. D. Myers  
Mr. D. Day

Aerospace Corp.  
Box 95085  
Los Angeles, Calif. 90045  
Attn: Mr. R. Hemden  
Mr. D. Hargis

Lockheed Missiles & Space Co.  
599 N. Mathilda Ave.  
Sunnyvale, Calif. 94088  
Attn: Dr. S. Adelfang  
Mr. C. Van der Moss

Lockheed Missiles and Space Co.  
Huntsville  
Res. & Engineering Center  
4800 Bradford Blvd.  
Huntsville, Ala. 35806  
Attn: Mr. R. DeMandel  
Mr. S. Krivo

Boeing Scientific Res. Lab.  
P. O. Box 3981  
Seattle, Wash. 98124  
Attn: Dr. Pao  
Library

The Boeing Co., Huntsville  
220 Wynn Dr.  
Huntsville, Ala. 35806  
Attn: Library

General Dynamics  
5873 Kearny Villa Rd.  
San Diego, Calif.  
Attn: Mr. F. Martin  
Library

North American Aviation, Inc.  
Space & Info. Systems Div.  
12214 Lakewood Blvd.  
Attn: Mr. C. D. Martin  
Mr. R. Lassen  
Library (2)

McDonald-Douglas  
Adv. Res. Labs.  
5251 Bolsa Ave.  
Huntington Beach, Calif. 92646  
Attn: Mr. J. Kelley  
Library (2)

Grumman Aircraft Engr. Corp.  
Bethpage, L. I., N. Y. 11714  
Attn: Library (2)

Martin-Marietta Corp.  
Aerospace Div.  
P. O. Box 179  
Denver 1, Col.  
Attn: Mr. J. M. Bidwell  
Library (2)

Bellcomm, Inc.  
1100 17th St. N. W.  
Washington, D. C. 20036  
Attn: Library (2)

Commander  
Hdqs., Air Weather Service  
Scott AFB, Ill. 62225  
Attn: Library (2)

Air Force Cambridge Res. Labs.  
Bedford, Mass. 01730  
Attn: Dr. H. Ohersten  
Tech. Library (5)  
Mr. N. Sissenwine (2)

Commander Base Weather Station (3)  
AFETR  
Patrick AFB, Fla. 32925

Air Force Flight Dynamics Lab.  
Air Force Systems Command  
Wright-Patterson AFB, Ohio  
Attn: Mr. G. Muller  
Mr. N. Loving  
Library

Atmospheric Sciences Lab. (2)  
U. S. Army Electronics Command  
White Sands Missile Range, New Mexico 88002

U. S. Army Missile Command  
Redstone Arsenal, Ala.  
Attn: Dr. O. Essenwanger  
Dr. O. Stewart  
Library

Commanding General  
U. S. Army Electronics Command  
Ft. Monmouth, N. J. 07703

Meteorology Division (2)  
U. S. Army Dugway Proving Ground  
Dugway, Utah 84022

Chief of Naval Res.  
Dept. of the Navy  
Washington, D. C. 20325

College of Earth & Mineral Sciences  
Pa. State Univ.  
University Park, Pa. 16802  
Attn: Dr. H. Panofsky  
Dr. J. Dutton  
Dr. H. Tennekes  
Dr. A. Blackadar

Dept. of Oceanography and Meteorology  
Texas A&M University  
College Sta. Texas 77840  
Attn: Dr. J. Scoggins

Dept. of Meteorology  
Univ. of Utah  
Salt Lake City, Utah 84116

Director  
Meteorology Dept.  
Univ. of Wash.  
Seattle, Wash. 99703

Dept. of Atmospheric Sciences  
Colorado State Univ.  
Ft. Collins, Colorado 80521  
Attn: Dr. E. Reiter

Dept. of Atmospheric Sciences  
Oregon State University  
Corvallis, Oregon 97330

Meteorology Dept.  
Fla. State Univ.  
Tallahassee, Fla. 32301  
Attn: Dr. Gleeson  
Dr. Hess

Meteorology Dept.  
New York Univ.  
University Heights  
New York, N. Y. 10001

Dept. of Earth Sciences  
University of Ala. Huntsville  
4701 University Drive 35805  
Attn: Dr. J. Branerd  
Dr. Shih

Dept. of Geosciences  
Purdue Univ.  
LaFayette, Ind. 47907  
Attn: Dr. Phil Smith

American Meteorological Society  
45 Beacon St.  
Boston, Mass. 02108

Federal Aviation Agency  
Washington, D. C. 20546

National Center for Atmospheric Res.  
Laboratory of Atmospheric Sci.  
Boulder, Colorado 80302  
Attn: Library (2)